Article:
Sanni, O, Bukuaghangin, O, Huggan, M et al. (3 more authors) (2017) Development of a novel once-through flow visualization technique for kinetic study of bulk and surface scaling. Review of Scientific Instruments, 88. 103903. ISSN 0034-6748

https://doi.org/10.1063/1.4991729

Development of a novel once-through flow visualization technique for kinetic study of bulk and surface scaling

O. Sanni, O. Bukuaghangin, M. Huggan, N. Kapur, T. Charpentier, and A. Neville

Citation: Review of Scientific Instruments **88**, 103903 (2017);
View online: https://doi.org/10.1063/1.4991729
View Table of Contents: http://aip.scitation.org/toc/rsi/88/10
Published by the American Institute of Physics

Development of a novel once-through flow visualization technique for kinetic study of bulk and surface scaling

O. Sanni,[1,a)] O. Bukuaghangin,[1] M. Huggan,[1] N. Kapur,[2] T. Charpentier,[3] and A. Neville[1]
[1]*School of Mechanical Engineering, Institute of Functional Surfaces, University of Leeds, Leeds, United Kingdom*
[2]*School of Mechanical Engineering, Institute of Thermofluids, University of Leeds, Leeds, United Kingdom*
[3]*School of Chemical and Process Engineering, University of Leeds, Leeds, United Kingdom*

(Received 22 June 2017; accepted 25 September 2017; published online 11 October 2017)

There is a considerable interest to investigate surface crystallization in order to have a full mechanistic understanding of how layers of sparingly soluble salts (scale) build on component surfaces. Despite much recent attention, a suitable methodology to improve on the understanding of the precipitation/deposition systems to enable the construction of an accurate surface deposition kinetic model is still needed. In this work, an experimental flow rig and associated methodology to study mineral scale deposition is developed. The once-through flow rig allows us to follow mineral scale precipitation and surface deposition *in situ* and in real time. The rig enables us to assess the effects of various parameters such as brine chemistry and scaling indices, temperature, flow rates, and scale inhibitor concentrations on scaling kinetics. Calcium carbonate ($CaCO_3$) scaling at different values of the saturation ratio (SR) is evaluated using image analysis procedures that enable the assessment of surface coverage, nucleation, and growth of the particles with time. The result for turbidity values measured in the flow cell is zero for all the SR considered. The residence time from the mixing point to the sample is shorter than the induction time for bulk precipitation; therefore, there are no crystals in the bulk solution as the flow passes through the sample. The study shows that surface scaling is not always a result of pre-precipitated crystals in the bulk solution. The technique enables both precipitation and surface deposition of scale to be decoupled and for the surface deposition process to be studied in real time and assessed under constant condition. *Published by AIP Publishing.* https://doi.org/10.1063/1.4991729

I. INTRODUCTION

The formation of calcium carbonate ($CaCO_3$) scale has been examined in many studies using different techniques which focus on the bulk solution or the deposition onto surfaces. Some studies have focused on comparisons between scale precipitation in the bulk solution and deposition on a surface. Such experiments have been carried out lately and this type of comparison seems to be critical for understanding scale formation.[1] The various techniques that have been used include the tube blocking tests,[2–4] bulk jar tests,[5] Quartz Crystal Microbalance (QCM),[6] Rotating Cylinder Electrode (RCE),[7] electrochemical methods, and modern dynamic techniques such as Synchrotron X-ray Diffraction (SXRD).[6–9] Analytical methods based on the electrochemical process were developed so as to quantify scaling.[7,10,11] Neville *et al.*[7] demonstrated that the extent of scale deposition on a metallic surface can be accurately estimated using analysis of the oxygen-reduction reaction at a rotating disk electrode (RDE) surface under potentiostatic control. A combined bulk chemistry/electrochemical measurement was later employed to study the precipitation, deposition, and inhibition of $CaCO_3$, thus enabling the precipitation and deposition kinetics to be compared and contrasted in the absence and presence of a commercial scale-control inhibitor.[12]

Much of the published work on inorganic scale has focussed on precipitation in a bulk solution and attempt to link it to thermodynamic precipitation models. There is not yet a full mechanistic understanding of how scale layers developed on solid surfaces because the kinetics of the bulk and surface processes are often different.[13] The scaling tendency for a given solution can be quantified by its saturation ratio (SR) which is the excess of the actual concentration of dissolved ions over the solubility product.[14–17] In many laboratory tests, the saturation ratio decreases with time as a result of reduction in ionic species as scale formation proceed, thereby making the development of a suitable surface kinetic model very difficult. To be able to predict scaling kinetics accurately, it is necessary to be able to quantify scaling as a function of the saturation ratio which should remain fairly constant at one point in the system. The inability to distinctively study bulk precipitation and surface deposition due to settling of particles as the size of scale crystals increases is also a major challenge. Non-electrochemical techniques such as quartz crystal microbalance (QCM) are not suitable to study later stages of crystallization.[6] The majority of the studies have focused on "off-line" or static conditions and the crystallization has not been recorded in real time.[18,19] In order to visualize the crystallization of calcium carbonate scale in real time, an electrochemical cell was used by Euvrard *et al.*[8] connected to a video setup; an optical assembly monitors and records the surface area of the working electrode during the experiment. It yielded some important information regarding the kinetics of scale formation induced by the application of a cathodic potential but deposition from a supersaturated solution was not considered. So far there has been one study which employed *in situ* methods for deposition from a supersaturated solution.[20]

[a)]Author to whom correspondence should be addressed: olujidesamuel@yahoo.com

The study was carried out in a closed *in situ* flow system where the saturation ratio was decreasing with time. Consequently, reduction in ionic species resulted in reduction in the driving force for scale formation.

Against this background, the present work is to design a flow system that enables the combined study of surface deposition and bulk precipitation scaling mechanisms and kinetics to be carried out while keeping the saturation ratio constant. A once-through visualization flow rig with associated image analysis procedure is developed to enhance the understanding of mechanisms as well as the relationship between scale surface deposition and bulk precipitation kinetics.

II. DESIGN OF A ONCE-THROUGH FLOW VISUALIZATION RIG

Control over scaling parameters is a prerequisite in order to fully understand the fouling process. In designing the rig, various combinations of scaling parameters such as composition of the feed (inlet supersaturation), residence time of solution in the flow cell, temperature of the bulk solution are systematically considered. The design is a once-through *in situ* rig system that enables longer experimental times to be considered as the saturation ratio remains constant at the working section where mineral scaling is evaluated. Fresh fluid of controlled supersaturation comes into contact with the sample, thereby avoiding the possible recirculation of preformed colloidal particles that may influence scale formation and complicate the analysis.

The flow rig setup consists of an *in situ* flow cell, a fibre optic turbidity probe, a high performance monochrome digital imaging device with 50 fps (frames per second) and 1 megapixel resolution, a thermocouple (type K), a double channel peristaltic digital pump used to allow pumping of the brines simultaneously, and an optima general purpose digital thermostatic circulator bath with a pump plastic tank, 15 °C–99 °C.

The flow cell is built of two polymethyl methacrylate (PMMA) plates [Figs. 1(a) and 1(b)], separated by chemically inert polytetrafluoroethylene (PTFE) gasket [Fig. 1(c)]. The first plate is 20 mm thick and houses the inlet and outlet of the channel with diameters of 5 mm each. The angle at the inlet and the outlet is equal to 20°. It also consists of two separate 20 mm diameter holes made through the plate. The first hole is to allow the surface being studied to be inserted. The second hole is for turbidity to be measured directly in the flow cell from a separate photometric glass window. The second plate is 5 mm thick consisting of two 20 mm diameter holes covered by glass windows allowing visualization of the flowing solution and of the surface located on the first plate. The dimensions of the cell channel made by the hole in the middle of the PTFE are 160 mm length, approximately, 40 mm wide, and 2 mm thick. The thickness enables the observation of the surface through the flow by the camera.

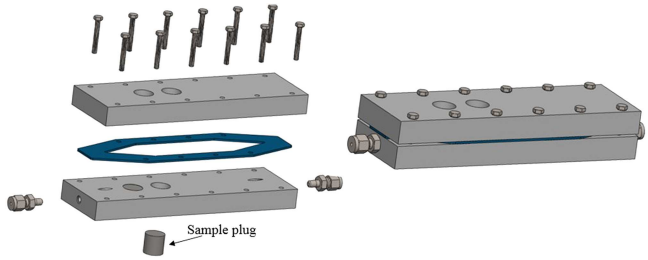

FIG. 2. *In situ* flow cell assembly.

The *in situ* flow cell assembly is presented in Fig. 2.

The *in situ* flow cell is designed for a laminar flow regime, and the hydrodynamic analysis of the cell at flow rates of 10 ml/min and 20 ml/min (Fig. 3) using computational flow dynamics (CFD) shows that there is no recirculation of flow, and more importantly, the flow velocity is uniform across the centre of the cell where the sample and turbidity measurements are taken.

A. *In situ* scale formation in flow rig

During a typical experiment, the separate solutions containing calcium and carbonate ions are pumped through the thermostatic water bath at the same flow rate and are maintained at the same temperature. The fluids are mixed together at the mixing unit close to the inlet of the *in situ* flow cell. The system is a once-through flow design such that the saturation ratio is constant as fresh brine continuously passes through the cell every time. The flow cell is designed to incorporate turbidity measurement and image capture of the metal surface very close to the point of mixing of the brine (Fig. 4). This helps to keep the residence time from mixing point to the sample below 5 s at 20 ml/min and also allows for a close comparative analysis of the bulk and surface mechanisms.

1. Surface visualization

The kinetic deposition of scale is followed in real time by a high performance digital camera connected to the computer.

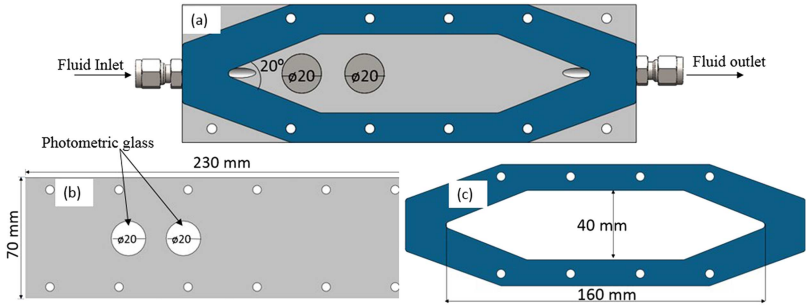

FIG. 1. *In situ* flow cell parts: (a) and (b) PMMA plates and (c) PTFE flow channel.

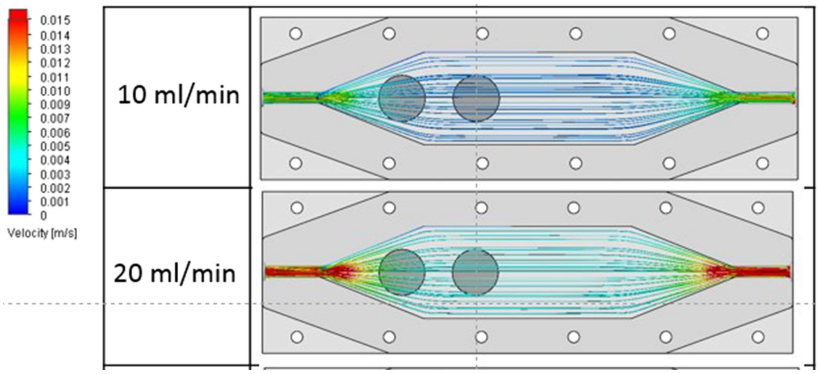

FIG. 3. Flow velocity field.

The camera allows accurate observations and instantaneous image capture of scale deposition on the steel in the removable plug inserted into the *in situ* flow cell (Fig. 2). The size of each frame after the lens is adjusted to give a good focus with minimum noise is 1 mm × 1 mm.

2. Turbidity measurement

The turbidity of the fluid is measured *in situ* in order to follow the bulk precipitation of the brine. A fibre optic turbidity probe is focused at an angle 90° to the photometric glass window. The light is transmitted through the glass to measure the turbidity of the solution in the cell and is reflected back by a mirror placed at the back of the cell. The turbidity is measured by light intensity that is reflected back into the probe.

III. EXPERIMENTAL SAMPLE PREPARATION

A. Brine chemistry

Five $CaCO_3$ scaling brine solutions with saturation ratio (SR) values of 10, 15, 25, 45, and 60 were used. For each brine solution, seawater (SW) and formation water (FW) were used and mixed at 50:50 mixing ratio. The compositions presented in Table I have been determined using the Multiscale™ software.

B. Material for surface deposition

For the study, a standard austenitic stainless steel UNS S31603 is used as the surface deposition material. The diameter of the samples on which deposition occurs is 1 cm, and the samples were carefully polished to achieve a very smooth surface of about 0.01 μm roughness.

TABLE I. Composition for $CaCO_3$ brine solution (mg/l) at 25 °C.

	NaCl		$NaHCO_3$		$CaCl_2 \cdot 2H_2O$	
SR	Brine 1	Brine 2	Brine 1	Brine 2	Brine 1	Brine 2
10	44.05	40.73	0.00	1.91	2.52	0.00
15	44.43	40.55	0.00	2.17	3.00	0.00
25	44.68	40.19	0.00	2.69	3.31	0.00
45	45.52	39.77	0.00	3.28	4.37	0.00
60	46.22	39.56	0.00	3.58	5.26	0.00

IV. IMAGE ANALYSIS PROCEDURE

The procedure for image analysis consists of a set of algorithms in the MATLAB programming language. They allow the image to be read as a matrix of pixels that are modifiable in order to improve the quality and extract the information needed. The procedure for image processing and analysis includes conversion to a binary image, thresholding, edge detection, morphological operations, and component labelling. The segmented image produced at the end of processing operations is assessed. Figure 5 shows the original image and the processed image which is analysed to assess the surface coverage of scale, the number, and average surface

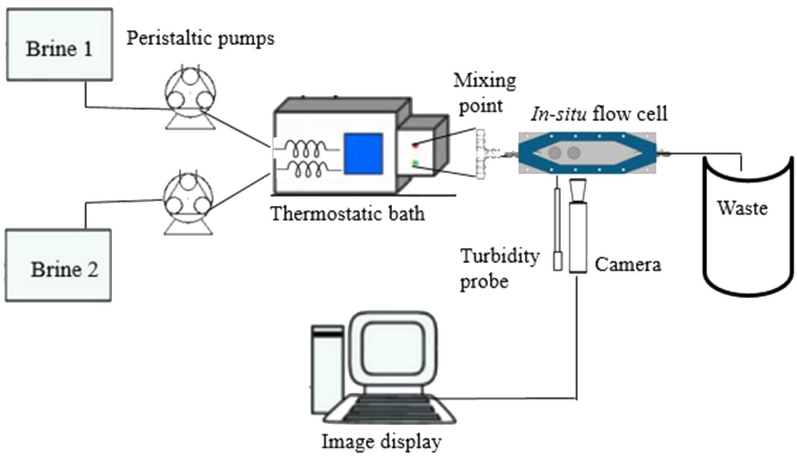

FIG. 4. Schematic diagram for the experimental flow rig.

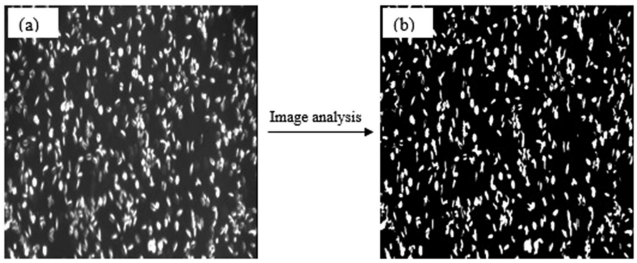

FIG. 5. (a) Original image and (b) processed image.

area of crystals. The detailed algorithm is presented in the supplementary material.

The number of crystals and the average area of crystals give information about the nucleation and growth processes, respectively, while the surface coverage gives the overall information regarding total scale deposited on the surface. As shown in Fig. 6, the repeatability of the test presented from at least 3 replicate experiments is good, and the results do not vary by more than 0.2 from the mean value.

V. EXPERIMENTAL RESULTS

A. Real time images of surface scale build-up: Morphology and internal crystal's structure

Scale formation on surfaces can be followed *in situ* and in real time with the high performance camera. Figure 7 shows images captured *in situ* with surface deposition process occurring for SR values of 45 at 25 °C. The increase in the number, average area, and surface coverage of crystals with time can be clearly observed and followed. This can be used to develop an understanding of nucleation and growth kinetics occurring at different experimental conditions.

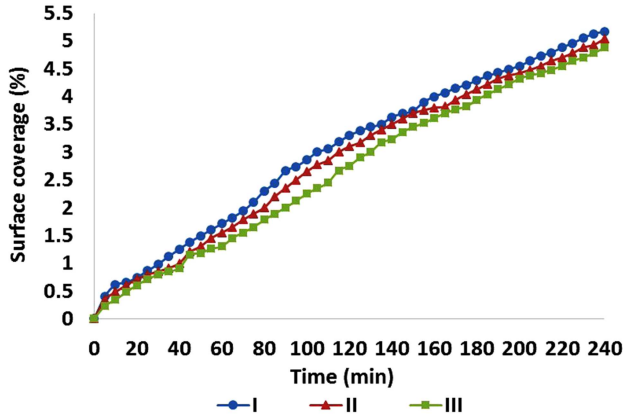

FIG. 6. Repeatability of the experimental procedure for three different tests; SR = 45, T = 25 °C.

SEM images of calcium carbonate scale formed on the surface at 25 °C, 40 °C, 60 °C, and 80 °C were taken to assess the morphology of the surface crystals formed on the samples in the *in situ* cell after 4 h. Figure 8 shows the SEM images for SR = 25 at 20 ml/min. Calcite predominates at low temperature. Vaterite is more stable at 40 °C, while the aragonite structure dominates at the higher temperature of 80 °C. This is in agreement with previous studies for bulk precipitation.[21–23] The observation is verified using X-ray diffraction (XRD).

The corresponding XRD patterns of the crystalline polymorphs for $CaCO_3$ at SR = 25 for 25 °C, 40 °C, 60 °C, and 80 °C are presented in Fig. 9. The diffraction peaks corresponding to aragonite are observed only at 80 °C, while only calcite peaks are observed at 25 °C. Calcite intensity is highest at 40 °C which represents the temperature at which vaterite peaks started to appear. Similar results have been observed in other studies.[8,24]

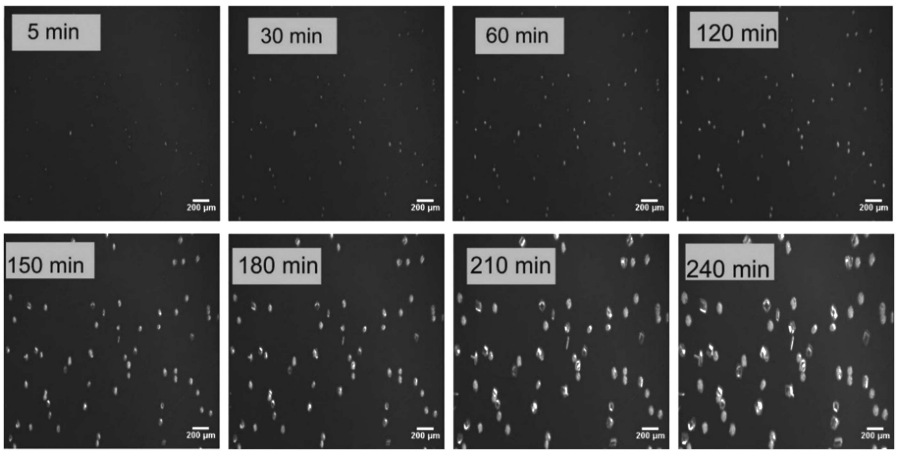

FIG. 7. *In situ* images of the $CaCO_3$ scale deposited on the surface with SR = 45 at 25 °C.

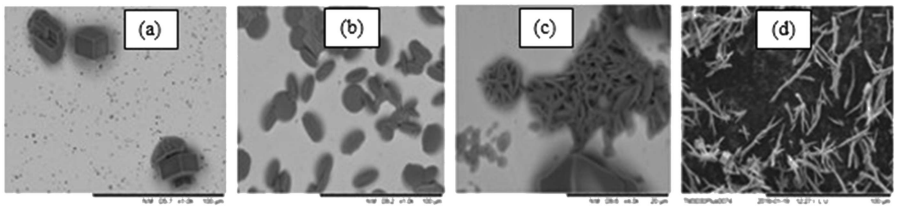

FIG. 8. SEM of $CaCO_3$ morphology at SR = 25, t = 4 h for (a) 25 °C, (b) 40 °C, (c) 60 °C, and (d) 80 °C.

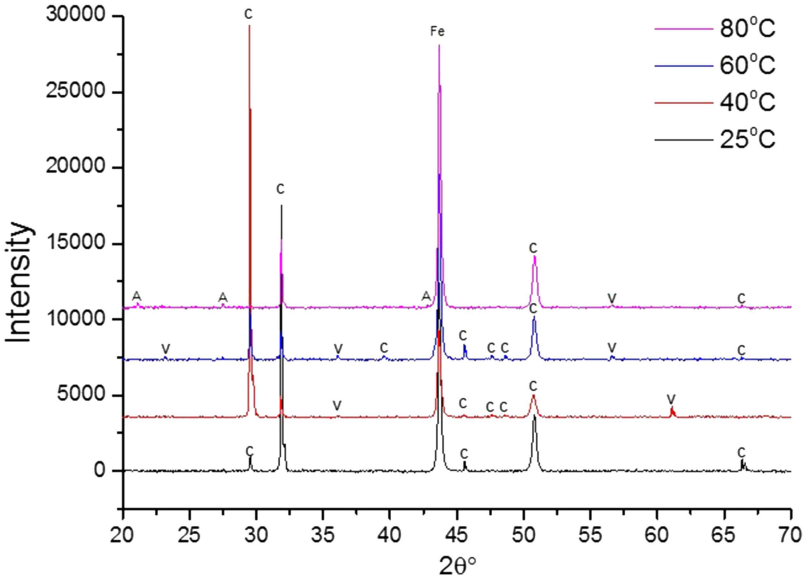

FIG. 9. Diffraction pattern of $CaCO_3$ scale for different temperatures at SR = 25.

B. Bulk precipitation and surface scaling

For the $CaCO_3$ brine with saturation ratio values of 10, 15, 25, 45, and 60, there are no detectable particles in the bulk solution for the entire duration of the test as the residence time from mixing of brine solution to the sample (~5 s) was shorter than the induction time for bulk precipitation to occur [Fig. 10(a)]. The images and turbidity measurement are recorded at 5 min interval for a duration of 4 h, and the corresponding surface images were processed using the image analysis procedures. The surface images which were taken adjacent to the turbidity and analysed show an increase in the surface coverage with time as seen in Fig. 10(b).

With zero turbidity indicating no detectable precipitated crystals in the bulk solution, the surface images as recorded from the *in situ* setup show crystals on the surface. The surfaces when removed from the flow cell and viewed with the scanning electron microscope (SEM) at the end of the deposition experiments show surface scale on the samples (Fig. 11). This is an important observation which confirms that in these conditions, the formation of scale on the surface is a surface crystallisation process rather than an adhesion process. This has important implications for the subsequent management of surface scaling.

Investigations carried out by Morizot and Neville[25] and Cheong *et al.*[26] suggested that heterogeneous surface

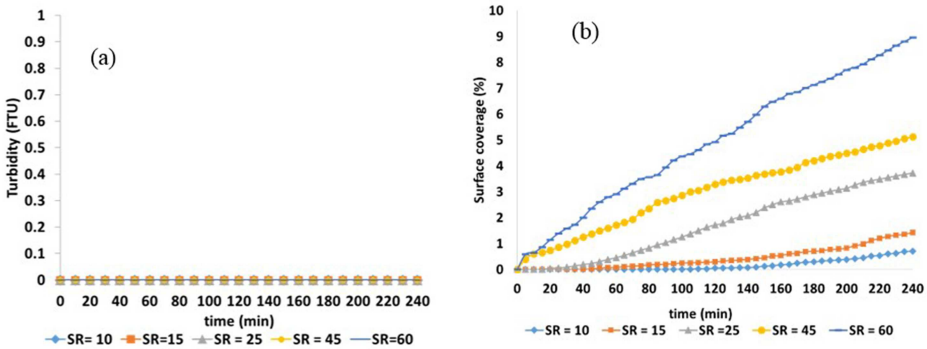

FIG. 10. (a) Bulk solution turbidity and (b) surface coverage of $CaCO_3$.

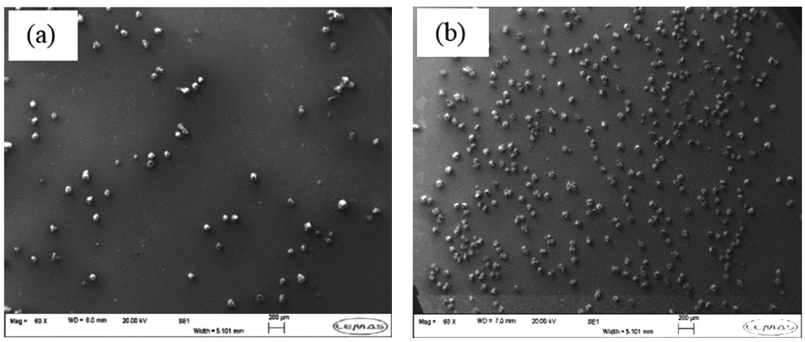

FIG. 11. SEM images of surface scale with no bulk precipitation at (a) SR = 25 and (b) SR = 60.

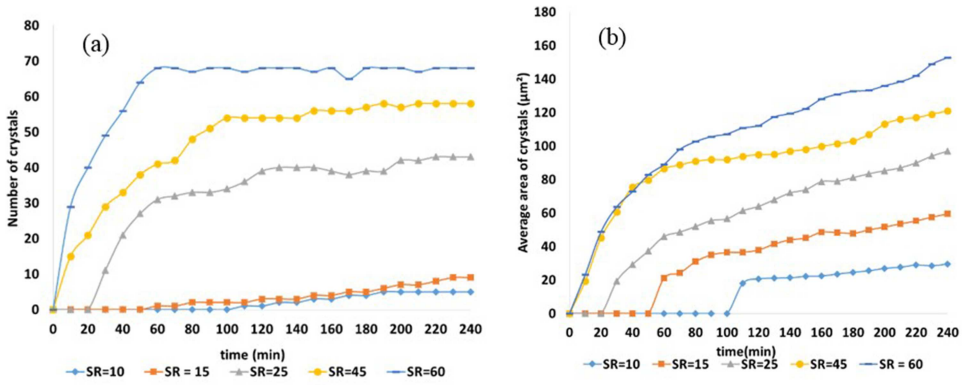

FIG. 12. (a) Number of crystals and (b) average crystal size for $CaCO_3$ at T = 25 °C for t = 4 h and 20 ml/min.

crystallisation and largely homogeneous precipitation are processes that should be isolated in the study of scaling. It is likely that using existing scaling indices for bulk precipitation, some caution should be taken when predicting surface scaling. It is essential to decouple the two processes to be able to distinctively study their mechanisms and kinetics and develop effective scale control strategies.

C. Quantification of surface nucleation and growth processes

The *in situ* visualization method used in this study has the capability to assess and quantify the overall scaling in terms of the nucleation and growth processes occurring on the sample surface. This is analysed by following the number and average area of crystals with time. Figure 12 shows the variation of the crystal size, and the numbers of crystals as a function of the saturation ratio.

From the plots, surface induction time can be observed for SR values of 10, 15, and 25 followed by nucleation and growth of the crystals. In all cases considered, the surface crystallization process seemed to reach a self-limiting number of crystals which is higher at higher values of SR [Fig. 12(a)]. This indicates that a surface may contain a finite number of active nucleation sites depending on the value of saturation ratio.[27] Regarding the trend of the curves for the average size of $CaCO_3$ crystals in Fig. 12(b), there is a continuous growth of crystals of the scale for the duration of the test due to the SR being kept constant as fresh brine passes across the samples.

In supersaturated environments, while the formation of many small crystals is kinetically favoured, the growth of large crystals is thermodynamically favoured. Based on the classical nucleation theory,[28] a nucleus must attain a critical size before it is stable and grow, otherwise, it will dissolve.

In a polynuclear system brought about by nucleation due to difference in induction time, the particles have various sizes distributed over the surface area as growth occurs progressively at the initial stage of crystallization (Fig. 13). The solubility difference between the polydispersed particles establishes a concentration gradient between the smaller and the larger particles, which leads to the growth of the larger particles at the expense of formation of new stable nuclei.[29,30] As such, depending on the concentration and movement of solvated ions to the surface, the growth of already stable crystals that are formed at the early stage of crystallization are favoured over the nucleation of new crystals. Improving the collective knowledge of surface deposition in terms of induction, nucleation, and growth processes will help in the application of an effective inhibition strategy and also in developing effective antifouling coatings to prevent scale formation on surfaces.[31–33]

D. Surface growth rate at constant saturation ratio

The early stages of the average area curve indicate the period of induction for the lower SR as well as the dominance of the nucleation process. The growth progresses linearly as no more new crystals are formed. Dawe and Zhang[34] showed that the plot of crystal size against time gives a straight line and the calcite layer growth rate can be determined from the slope of this straight line. Hasson *et al.*[35] also measured the rate of scale growth under the condition such that the scale layers grow linearly with time. The surface

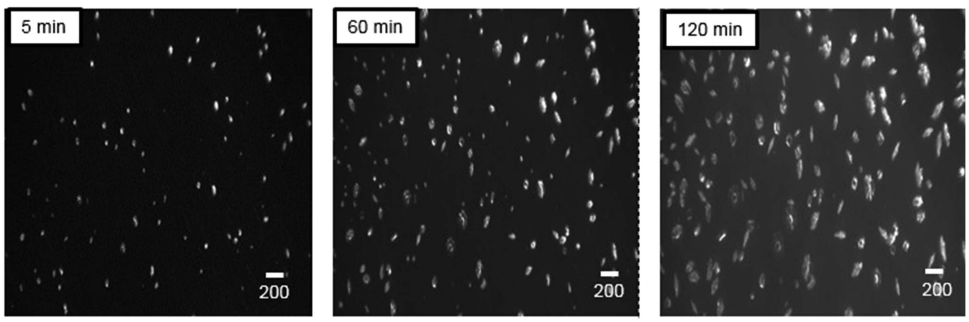

FIG. 13. Nucleation and growth of particles on the surface.

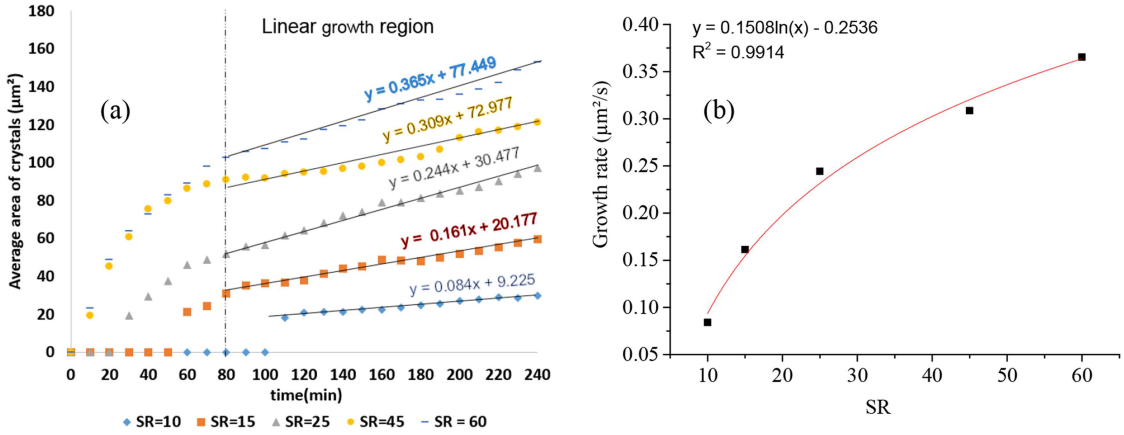

FIG. 14. (a) Average crystal size and (b) surface growth rate as a function of saturation ratio (SR).

growth rates for SR 10, 15, 25, 45, and 60 were determined by a linear fit after the induction period in the plot of average size of crystals versus time [Fig. 14(a)]. The plot of growth rate as a function of SR gives a logarithmic relationship as shown in Fig. 14(b). The relationship between the growth rates and supersaturation is used to indicate the growth mechanisms.[36,37]

Previous assessments of deposition rate[38–41] were based on initial rate constant and initial SR because of the decrease in concentration of ions with time, whereas, in the field, it is likely that a surface is exposed to the same condition for a fairly long time. Euvrard *et al.*[42] observed a lateral growth rate of $CaCO_3$ which decreases as the degree of supersaturation ratio decreases. In other studies, growth rates with a linear dependency on the SR were obtained at higher SR with high growth rates controlled by the diffusion and adhesion of particles from the bulk solution.[36] The rate is controlled by the transport of the ions in the bulk solution or by the adsorption process. However, the model in this study fits the exponential growth rate which describes a crystallization mechanism involving a surface nucleation determining step.[36] The plot of the rate of growth as a function of the logarithm of the relative supersaturation is shown in Fig. 15. Sparingly soluble electrolytes mostly grow by a logarithmic or exponential rate law at small or moderate supersaturations and may change to transport control at larger concentrations.[37]

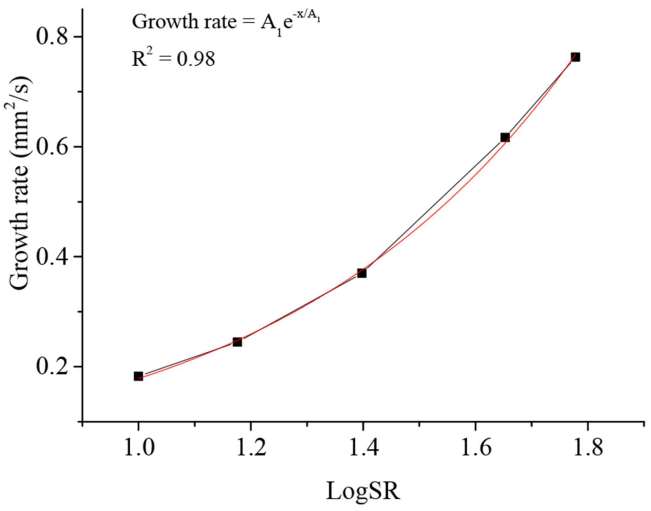

FIG. 15. Growth rate as a function of Log SR.

In the range of SR (10–60) considered for this study, deposition is initiated by heterogeneous nucleation on the surface and subsequent growth of isolated crystals. Most of the previous studies to predict kinetics have been based on bulk scaling experimentation and significantly less is known about the $CaCO_3$ crystal formation rate on a solid surface at constant SR. This is important in order to move towards predictions and proper assessment of kinetics.

VI. CONCLUSION

The newly developed methodology offers new insights into surface fouling kinetics of sparingly soluble salts. The setup allow us to decouple homogeneous bulk precipitation and heterogeneous surface crystallization in order to assess more accurately the role played by adhesion and crystallization on build-up of calcium carbonate under constant experimental conditions. Within the range of saturation ratio considered, it is shown that mineral scale build-up is not always a result of adhesion of pre-precipitated crystals from bulk solution but can also be driven by heterogeneous surface crystallization. At the lower saturation ratio considered, calcium carbonate deposition at the early stage is strongly affected by the slow progressive nucleation rate of crystals with growth of already stable crystals occurring simultaneously. At a higher saturation ratio, the nucleation rate of crystals is fast; thus, no measurable induction period was observed. In all cases, the density of calcium carbonate crystals reaches a plateau and the later stages of surface fouling are solely driven by the growth of crystals. As such, fouling is affected by the state of the substrate onto which the deposition proceeds as well as the saturation ratio of the scaling solution. This setup allows us to clearly study and understand the nucleation and growth processes taking place on surfaces; it has applications for the development of novel and more effective mineral scale inhibition strategy, targeting either a nucleation or growth inhibition depending on the experimental conditions.

SUPPLEMENTARY MATERIAL

See supplementary material for the algorithm on image analysis and the real time visualization rig.

ACKNOWLEDGMENTS

The authors would like to appreciate the Flow Assurance and Scale Team (FAST) and Petroleum Technology Development Fund for their support and contributions to the success of the study.

[1]D. Hasson *et al.*, "Influence of the flow system on the inhibitory action of $CaCO_3$ scale prevention additives," Desalination **108**(1-3), 67–79 (1997).
[2]Y. Zhang *et al.*, "The kinetics of carbonate scaling—Application for the prediction of downhole carbonate scaling," J. Pet. Sci. Eng. **29**(2), 85–95 (2001).
[3]W. Frenier and M. Ziauddin, *Formation, Removal, and Inhibition of Inorganic Scale in the Oilfield Environment* (Society of Petroleum Engineers, 2008).
[4]S. Dyer and G. M. Graham, "The effect of temperature and pressure on oilfield scale formation," J. Pet. Sci. Eng. **35**, 95–97 (2002).
[5]A. L. Graham *et al.*, "How minimum inhibitor concentration (MIC) and sub-MIC concentrations affect bulk precipitation and surface scaling rates," in *SPE International Symposium on Oilfield Chemistry* (Society of Petroleum Engineers, Inc., The Woodlands, Texas, 2005).
[6]C. Gabrielli *et al.*, "Quartz crystal microbalance investigation of electrochemical calcium carbonate scaling," J. Electrochem. Soc. **145**, 2386–2396 (1998).
[7]A. Neville *et al.*, "Electrochemical assessment of calcium carbonate deposition using a rotating disc electrode (RDE)," J. Appl. Electrochem. **29**(4), 455–462 (1999).
[8]M. Euvrard, C. Filiatre, and E. Crausaz, "Cell to study *in situ* electrocrystallization of calcium carbonate," J. Cryst. Growth **216**(1), 466–474 (2000).
[9]G. H. Nancollas, "Kinetics of crystal growth from solution," J. Cryst. Growth **3-4**(C), 335–339 (1968).
[10]C. Gabrielli *et al.*, "Nucleation and growth of calcium carbonate by an electrochemical scaling process," J. Cryst. Growth **200**(1-2), 236–250 (1999).
[11]J. Rinat *et al.*, "Electrocrystallization of calcium carbonate on carbon-based electrodes," J. Electroanal. Chem. **575**(2), 195–202 (2005).
[12]A. Neville *et al.*, "A combined bulk chemistry/electrochemical approach to study the precipitation, deposition and inhibition of $CaCO_3$," Chem. Eng. Sci. **55**(20), 4737–4743 (2000).
[13]W. F. Langlier, *The Analytical Control of Anti-Corrosion Water Treatment* (The American Water Works Association, 1936), Vol. 28, pp. 1500–1521.
[14]R. M. Pytkowicz, "Rates of inorganic calcium carbonate nucleation," J. Geol. **73**(1), 196–199 (1965).
[15]T. Chen *et al.*, "Assessing the effect of Mg^{2+} on $CaCO_3$ scale formation–bulk precipitation and surface deposition," J. Cryst. Growth **275**, e1341–e1347 (2004).
[16]P. R. Roberge, *Handbook of Corrosion Engineering* (McGraw-Hill, 2000).
[17]A. G. Walton, *The Formation and Properties of Precipitates* (Interscience Publishers, New York, 1967).
[18]N. Abdel-Aal, K. Satoh, and K. Sawada, "Study of the adhesion mechanism of $CaCO_3$ using a combined bulk chemistry/QCM technique," J. Cryst. Growth **245**(1-2), 87–100 (2002).
[19]T. Chen *et al.*, "Calcium carbonate scale formation—Assessing the initial stages of precipitation and deposition," J. Pet. Sci. Eng. **46**(3), 185–194 (2005).
[20]V. Eroini, "Kinetic study of calcium carbonate formation and inhibition by using an *in situ* flow cell," Ph.D. thesis, University of Leeds, 2012.
[21]Y. Kitano, "A study of the polymorphic formation of calcium carbonate in thermal springs with an emphasis on the effect of temperature," Bull. Chem. Soc. Jpn. **35**, 1980–1985 (1962).
[22]Y. S. Han *et al.*, "Factors affecting the phase and morphology of $CaCO_3$ prepared by a bubbling method," J. Eur. Ceram. Soc. **26**(4-5), 843–847 (2006).
[23]M. Kitamura, "Controlling factor of polymorphism in crystallization process," J. Cryst. Growth **237-239**(Part 3), 2205–2214 (2002).
[24]P. Kjellin, "X-ray diffraction and scanning electron microscopy studies of calcium carbonate electrodeposited on a steel surface," Colloids Surf., A **212**(1), 19–26 (2003).
[25]A. P. Morizot and A. Neville, "Using an electrochemical approach for monitoring kinetics of $CaCO_3$ and $BaSO_4$ scale formation and inhibition on metal surfaces," SPE J. **6**(2), 220–223 (2001).
[26]W. C. Cheong, P. H. Gaskell, and A. Neville, "Substrate effect on surface adhesion/crystallisation of calcium carbonate," J. Cryst. Growth **363**, 7 (2012).
[27]L. Beaunier *et al.*, "Investigation of electrochemical calcareous scaling: Nuclei counting and morphology," J. Electroanal. Chem. **501**(1-2), 41–53 (2001).
[28]J. W. Mullin, *Crystallization*, 4th ed. (Butterworths, London, 2001).
[29]M. Kahlweit, "Ostwald ripening of precipitates," Adv. Colloid Interface Sci. **5**(1), 1–35 (1975).
[30]R. D. van der Weijden *et al.*, "The influence of total calcium and total carbonate on the growth rate of calcite," J. Cryst. Growth **171**(1), 190–196 (1997).
[31]A. Neville, "Surface scaling in the oil and gas sector: Understanding the process and means of management," Energy Fuels **26**(7), 4158–4166 (2012).
[32]T. V. J. Charpentier *et al.*, "Liquid infused porous surfaces for mineral fouling mitigation," J. Colloid Interface Sci. **444**, 81–86 (2015).
[33]M. M. Vazirian *et al.*, "Surface inorganic scale formation in oil and gas industry: As adhesion and deposition processes," J. Pet. Sci. Eng. **137**, 22–32 (2016).
[34]R. A. Dawe and Y. Zhang, "Kinetics of calcium carbonate scaling using observations from glass micromodels," J. Pet. Sci. Eng. **18**(3-4), 179–187 (1997).
[35]D. Hasson *et al.*, "Mechanism of calcium carbonate scale deposition on heat-transfer surfaces," Ind. Eng. Chem. Fundam. **7**(1), 59–65 (1968).
[36]E. M. Flaten, M. Seiersten, and J.-P. Andreassen, "Growth of the calcium carbonate polymorph vaterite in mixtures of water and ethylene glycol at conditions of gas processing," J. Cryst. Growth **312**(7), 953–960 (2010).
[37]A. E. Nielsen, "Electrolyte crystal growth mechanisms," J. Cryst. Growth **67**(2), 289–310 (1984).
[38]F. A. Setta, A. Neville, and H. J. Chen, "A surface kinetic scaling model for $CaCO_3$ on a stainless steel surface (316 L)," Corrosion International 285–303 (2012).
[39]A. J. Karabelas, "Scale formation in tubular heat exchangers—Research priorities," Int. J. Therm. Sci. **41**(7), 682–692 (2002).
[40]M. G. Lioliou *et al.*, "Heterogeneous nucleation and growth of calcium carbonate on calcite and quartz," J. Colloid Interface Sci. **308**(2), 421–428 (2007).
[41]E. M. Flaten, M. Seiersten, and J.-P. Andreassen, "Induction time studies of calcium carbonate in ethylene glycol and water," Chem. Eng. Res. Des. **88**(12), 1659–1668 (2010).
[42]M. Euvrard *et al.*, "Kinetic study of the electrocrystallization of calcium carbonate on metallic substrates," J. Cryst. Growth **291**(2), 428–435 (2006).